Supplementary Materials: The Synergy Effect of Ni-M (M = Mo, Fe, Co, Mn or Cr) Bicomponent Catalysts on Partial Methanation Coupling with Water Gas Shift under Low H_2/CO Conditions

Xinxin Dong, Min Song, Baosheng Jin, Zheng Zhou and Xu Yang

S1. Experimental Setup

Figure S1 provides a detailed experimental setup, including units of gas supplying, reaction controlling, catalytic reacting, gas sampling and gas analyzing. For the gas supplying unit, the mixed reactant dry gas was prepared from the individual gases controlled by mass flow meters (Sevenstar, Beijing, China), and the required steam was supplied by a steam generator. For the catalytic reacting unit, the reaction was performed in a continuous fixed-bed reactor equipped with a stainless steel tube (inner diameter: 50 mm; length: 1000 mm) at atmospheric pressure. A 600-mm *K*-type thermocouple situated in the middle of the catalyst bed was utilized to measure the reaction temperature. To deter the condensation of the generated steam, the pipe between the reactor and the steam generator was wrapped up with a heating belt. As for the gas sampling and gas analyzing unit, the outlet gas stream was cooled down by a cold trap, and the residual water was removed by abundant allochroic silica gel, lest it deteriorate the separation columns of the gas chromatograph. The purified outlet gas was collected by a gas bag and analyzed by gas chromatography.

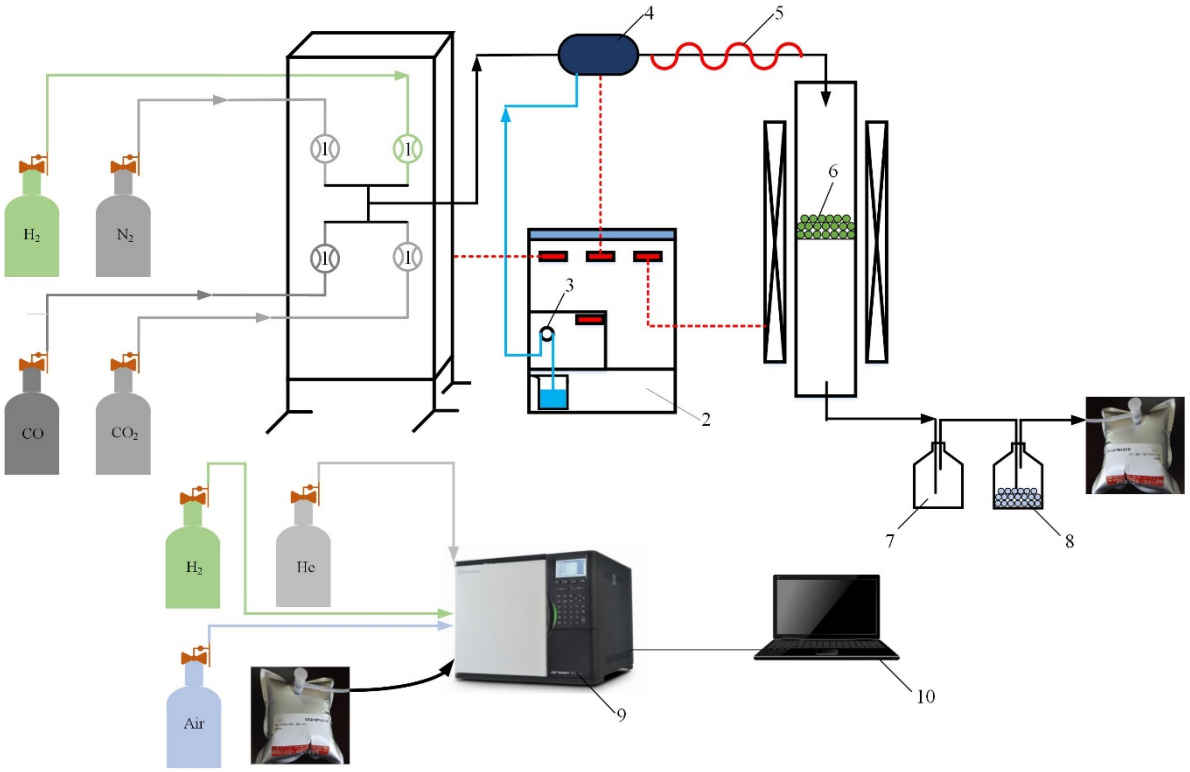

1. Mass Flow Meter 2. Control Panel 3. Peristaltic Pump 4. Steam Generator 5. Heating Belt
6. Catalysts 7. Cold Trap 8. Allochroic Silica Gel 9. Gas Chromatography 10. Workstation

Figure S1. Schematic diagram of the catalyst testing.

S2. Nitrogen Adsorption Analysis

Figure S2 displays the nitrogen adsorption-desorption isotherms and the pore size distribution (PSD) curves of the support and as-prepared catalysts. As can be seen from Figure S2A, all isotherms belong to type IV according to the IUPAC (International Union of Pure and Applied Chemistry) classifications for the isotherms, indicating the support and as-prepared catalysts have a mesoporous structure (2–50 nm). In addition, a decrease in the steepness of the capillary condensation step can be observed when Ni and/or the second metal is added on the support, revealing the decrease of mesoporous uniformity [1]. As shown in Figure S2B, the pore size distribution (PSD) curves of all samples exhibit only one narrow peak, confirming to some extent the uniformity of the channels.

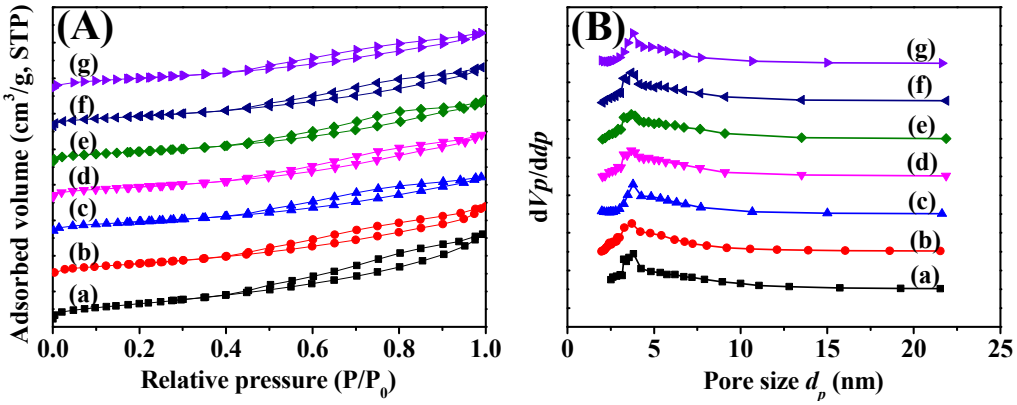

Figure S2. N_2 adsorption isotherms (**A**) and pore size distribution (PSD) curves (**B**) of the support and as-prepared catalysts: (a) γ-Al_2O_3, (b) 15Ni, (c) 15Ni-3Mo, (d) 15Ni-3Fe, (e) 15Ni-3Co, (f) 15Ni-3Mn and (g) 15Ni-3Cr.

S3. XRD Analysis

Figure S3 presents the XRD patterns of the γ-Al_2O_3 support with/without calcination. As can be seen, the fresh support (a) exhibits a mixed pattern of γ-Al_2O_3 at 2θ = 37.4, 45.8 and 67.3° (PDF#04-0880) and AlO(OH) at 2θ = 14.5, 28.2, 32.1, 48.9 and 72.0° (PDF#74-1895) instead of the characteristics of pure γ-Al_2O_3. The large specific surface area of the γ-Al_2O_3 support (Table 1) leads to a considerable amount of water vapor in the air being adsorbed, thus transforming part of the support into AlO(OH) through the $Al_2O_3 + H_2O \rightarrow 2AlO(OH)$ reaction. This type of alkaline surface is beneficial for the bonding with acidic nitrate precursors and, as a result, increases the impregnation efficiency. For comparison, the XRD patterns of the calcined support (b) mainly show simplex peaks ascribed to γ-Al_2O_3, except tiny AlO(OH) peaks at 2θ = 14.5, 28.2°, possibly due to the adsorption of vapor in the air during sample preparation for XRD analysis.

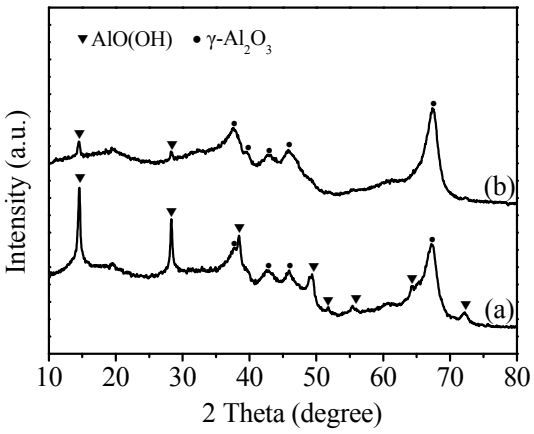

Figure S3. X-ray diffractogram (XRD) patterns of the γ-Al_2O_3 support: (**a**) before calcination and (**b**) after calcination at
450 °C for 4 h.

S4. H_2-TPR Analysis

Table S1. Detailed data of the deconvolved TPR profiles.

Samples	T_p (°C)			Fraction (%)			Proportion of α Plus β (%)
	α	β	γ	α	β	γ	
15Ni	435	568	681	26	36	38	62
15Ni-3Mo	427	490	650	23	37	40	60
15Ni-3Fe	340	524	679	30	35	35	65
15Ni-3Co	432	571	693	35	35	30	70
15Ni-3Mn	464	587	694	25	41	34	66
15Ni-3Cr	473	572	682	34	38	28	72

S5. SEM Analysis

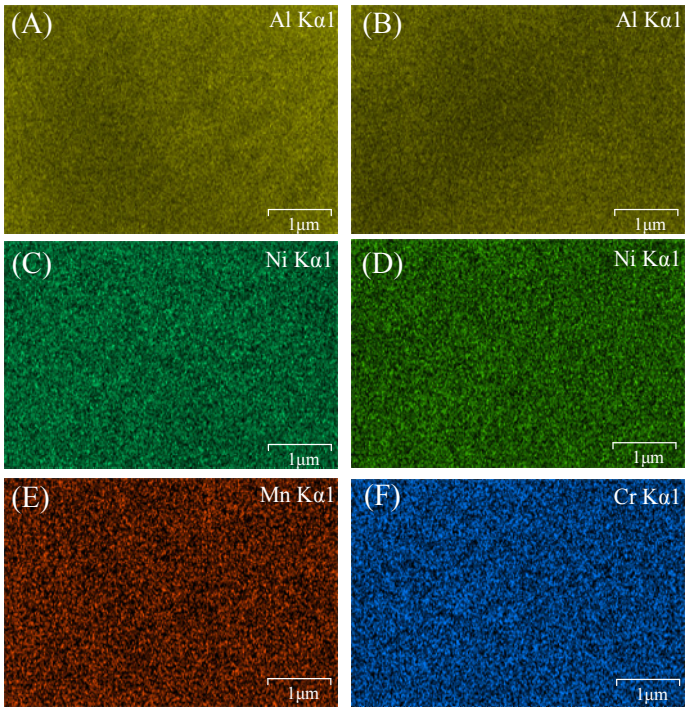

Figure S4. Elemental mapping images of reduced catalysts: (**A**,**C**,**E**) 15Ni-3Mn; (**B**,**D**,**F**) 15Ni-3Cr.

S6. Effect of Mn Loading

As can be seen in Figure S5, the CH_4 content increases and the CO content decreases the first time with the Mn amount, while after 3 wt % of Mn loading, the CH_4 content decreases and the CO content increases with the Mn amount, indicating that the synergy effect is closely related with the amount of Mn addition. With insufficient MnO_x species, the 15Ni catalyst shows a relatively low activity for CO methanation and a poor synergy effect for WGS. However, the excess of Mn loading would cover some of the Ni active sites, thus decreasing the H_2 chemisorption ability [2]. As a consequence, proper loading of Mn is the key to cause the optimal synergy effect between Ni and MnO_x species.

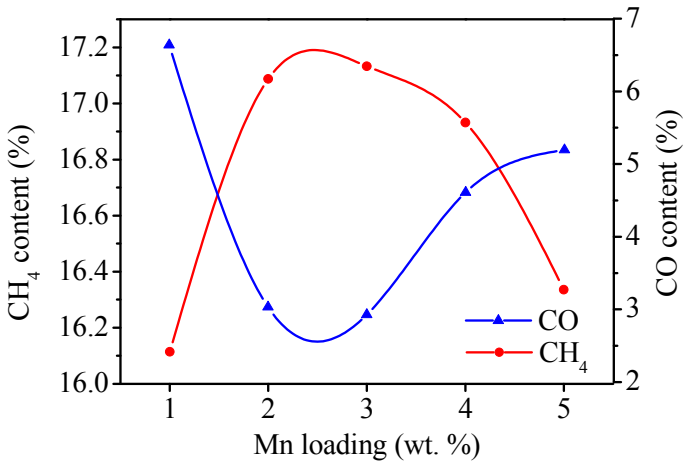

Figure S5. Effect of Mn loading in 15Ni catalyst on the partial methanation coupling with WGS at 350 °C, $H_2/CO = 0.8$ and $H_2O/CO = 1$.

References

1. Liu, Q.; Zhong, Z.; Gu, F.; Wang, X.; Lu, X.; Li, H.; Xu, G.; Su, F. CO methanation on ordered mesoporous Ni–Cr–Al catalysts: Effects of the catalyst structure and Cr promoter on the catalytic properties. *J. Catal.* **2016**, *337*, 221–232.
2. Lu, X.; Gu, F.; Liu, Q.; Gao, J.; Jia, L.; Xu, G.; Zhong, Z.; Su, F. Ni–MnO_x Catalysts Supported on Al_2O_3-Modified Si Waste with Outstanding CO Methanation Catalytic Performance. *Ind. Eng. Chem. Res.* **2015**, *54*, 12516–12524.